On Down-Scaled Modelling of Wind Turbine Drivetrains

On Down-Scaled Modelling of Wind Turbine Drivetrains

Geraldo F. de S. Rebouças, Amir R. Nejad

Department of Marine Technology
Norwegian University of Science and Technology – NTNU
NO-7491, Trondheim, Norway

E-mail: Geraldo.Reboucas@ntnu.no

Abstract. Gearbox testing is an important and complex task that will become even more challenging as the wind industry moves towards ever-growing turbines. The burden of this task can be decreased by using reduced-scale models with similar characteristics as its industrial-scale equivalent. This work presents a step-by-step procedure to down-scale a gearbox to different fractions of its rated power while preserving its core properties: structural safety and frequency distribution. The parameters to be scaled are sub-divided according to their relation to the system's integrity and dynamic behavior. After performing an overall scaling, it is possible to fine-tune the scaling factors, according to the user precision requirements. Simulations show that it is possible to down-scale a gearbox to 0.01 % of its rated power while having less than 10 % relative deviation on its pitting safety factor. These preliminary results show that wind turbine drivetrain testing can become more affordable by using down-scaled models in a structured manner.

1. Introduction

Nowadays, wind turbine gearboxes (WTGs) are mainly tested at full scale in third party expensive specialized facilities, with ever-growing capabilities [1, 2, 3]. Those tests tend to become even more restrictive and demanding as the size, height, and power of wind turbines (WT) keeps growing continuously with no signs of stagnation in the next years [4]. Industry wants to decrease costs with the use of WTs with more than 10 MW capacity, leading to bigger and more complex drivetrains.

Despite the advances in computational power in the last decades, experiments continue to provide valuable insights to improve or develop new products. Sub-scaled models are known for enabling time and money-saving tests [5] and have been used for fluid and structural aspects of wind turbines [6, 7], but are rarely applied to machinery, considering only over-simplified models.

A design methodology for developing a reduced-scale test rig for condition monitoring purposes is presented in [8], having a roped elevator as a reference application. The similarity between reference and scaled systems is ensured using dimensional analysis (DA) and evaluated through simulations and experiments. Scaling laws for the main parameters of an elevator are used to derive scaling relations for the others. Parameter ranges are defined based on different elevator installations and to make the test rig compact. Kinematic ranges were freely defined by the authors. Specific scaled models were generated using least squares based on different configurations of the elevator, e.g. varying the number of floors and/or applied load.

To realize time-accelerated experiments in a wind energy conversion system, Varais et al. [9] developed a hardware in the loop simulation system using DA. Experiments showed that it is possible to establish connections between several scaled models, underlining the possibility of accelerating tests using information from similitude factors.

In [10], a 3.5 kW test rig is designed to emulate the torque response of a 2 MW WT (0.175 %) in terms of a similar time constant and wind speed range for optimal tip speed ratio (TSR). The main design parameters were the rotor radius and the flywheel mass moment of inertia, which were determined using data from commercial 3 kW small WTs. The same test rig was used in [11] to investigate its similarity to a 2 MW WT in terms of the pitch response. In both works, the outputs of interest for the test rig and WT have the same magnitude, despite the power scaling.

To decrease risk in full-scale commercial projects, the model testing of a down-scaled (12.5 %) floating WT using Froude-scale model testing techniques is presented in [6], highlighting the need for proper scaling techniques. Challenges to implementing the scaled model occurred due to opposing design requirements. The scaled model was designed using similar materials and procedures of a 6 MW WT (0.33 %). Although the authors claimed that their data could be used to validate the full-scale system, there were no comparisons between down and full-scale WTs, nor explanations on how to do such validation.

To verify advanced diagnosis algorithms, a down-scaled hardware simulator of a WT was developed and presented in [12], following the characteristics of a 3 MW WT (0.66 % scaling). The simulator gearbox has the same configuration as the full-scale WT, and the scaled blade was designed to have the same characteristics as its full-scale counterpart. Experimental results show a qualitative similarity between the responses of the simulator and full-scale WT, although there was no information on how to estimate the WT response from its simulator, nor a clear design procedure to ensure the similarity between their outputs of interest.

From this overview one can see that although reduced-scale models are being used in different contexts of the wind industry, there are only specific scale comparisons, showing the lack of wide range scaling methodologies, specially for drivetrains. Reduced scale prototypes leads to affordable experiments. They can be used to test new condition monitoring and fault detection methods, new drivetrain technologies, components and materials. The development of a structured wide-range scaling procedure is essential to extend the results of reduced-scale tests to industrial drivetrains.

Thus, the main objective and originality of this work is the development of a procedure to down-scale a WT drivetrain while having limited variations on its structural integrity and natural frequency distribution. The complexity of the down-scaling problem is decreased by arranging the parameters to be scaled in groups, performing an overall scaling that can be fine-tuned in later steps, according to the user needs. Positive and challenging aspects of the developed procedure are discussed. This work shows how a 5 MW WTG can be down-scaled to 0.01 % of its rated power with minimum variations of its core properties. The resulting procedure to develop down-scaled lab prototypes can be used to decrease the costs of testing existing and novel equipment through the systematic use of reduced-size versions of large-scale industrial drivetrains.

2. Drivetrain scaling

In this work, the reference system is the gearbox proposed by [13] as the reference gearbox for the NREL 5 MW WT. It consists of three stages (2 planetary and 1 parallel), as shown in Fig. 1. The scaled and reference versions of the drivetrain must have the same level of structural integrity and similar spacing between resonances. That must be done without modifying the gearbox's configuration or material composition. The structural integrity is measured in terms of contact stresses (ISO 6336-2 [14]) for the gear pairs and fatigue and yield stresses [15] for the shafts.

Only the torsional dynamics of the gearbox is considered in this work, with the shafts acting as springs between inertial elements (rotor, generator and gear stages). The internal torsional

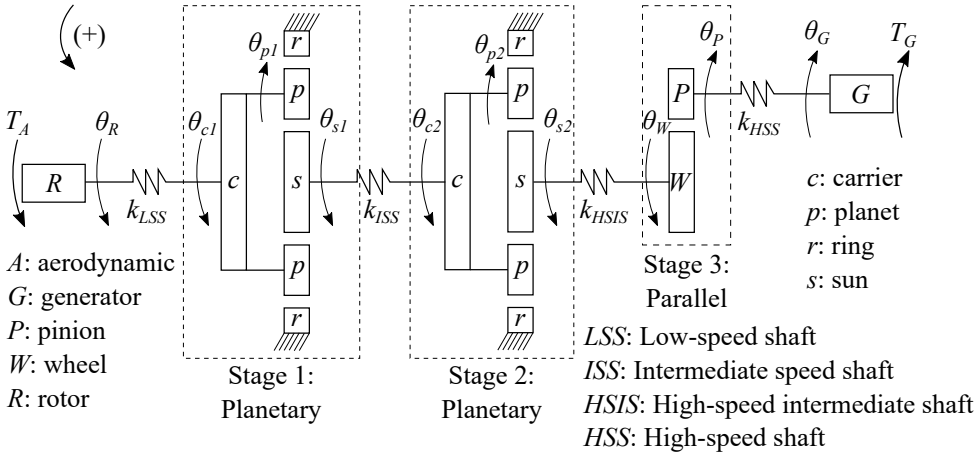

Figure 1: Lumped parameter representation of the NREL 5 MW drivetrain.

dynamics of each gear stage is modeled according to [16], where each planetary stage has 5 degrees-of-freedom (DOFs) (carrier, 3 planets, and sun) and the parallel stage has two DOFs. Considering that the rotor and generator have one DOF each, the full system has 14 DOFs and its inertia matrix is a function of the gear scaling factors together with the rotor, generator and shafts mass moment of inertia. The stiffness matrix is governed by the scaling factors for the shafts (length and diameter) and gear pairs (meshing stiffness). The mass and stiffness matrices can be found in the Appendix.

The main input for the scaling process is the rated power P because it is the defining parameter of every WT. The rated rotor speed n is kept constant, but it could be a second input for the scaling process or it could be scaled in order to preserve the reference system TSR using similarity laws [7]. The parameters to be scaled are the gear's normal module m_n and face width b at each stage, the shaft's length L and diameter D, and the rotor and generator mass moment of inertia J. The variation of the mass moment of inertia of a body whose dimensions were scaled can be understood by remembering that J has units of mass times length squared and that the mass of a body can be written as the product of its density and volume (length to the third power). Therefore, when scaling the dimensions of a body by a factor γ, its mass moment of inertia will be scaled by γ^5.

Keeping a constant stress level for scaled and reference shafts and neglecting radial loads, one can show that the scaling factor of the shaft diameter γ_D must be proportional to the cubic root of the applied torque scaling factor:

$$\sigma \propto \frac{T}{D^3} \Rightarrow \gamma_\sigma = \frac{\gamma_T}{\gamma_D^3} = 1,$$
$$\gamma_D = \gamma_T^{1/3}, \tag{1}$$

where γ_σ, γ_T, and γ_D are the scaling factors for the parameters σ, T and D, representing principal stress, applied torque, and shaft diameter, respectively. Knowing that the rated power P is proportional to the product between the applied torque T and the shaft's speed n, which is constant for scaled and reference systems ($\gamma_n = 1$), one arrives at:

$$\gamma_D = \gamma_P^{1/3}. \tag{2}$$

The shaft's length does not influence the stresses because only torsional loads are considered. This parameter, together with the mass moment of inertia of the rotor and generator will have

an influence only on the system's resonances, which will be affected indirectly by the other parameters to be scaled. For instance, the normal module and face width affect the meshing stiffness and the mass moment of inertia of the gears.

Roughly speaking, this work aims at developing down-scaled gearboxes with smaller dimensions than its reference counterpart. If the reference and scaled gearboxes have resonances with the same value, the mass decrease should be followed by an equal stiffness decrease, leading to longer shafts and going against the objective of this work. Thus, normalized resonances are used instead, leading to systems with similar frequency distribution. The i-th normalized resonance $\bar{f}_{n,i}$ is obtained by dividing the i-th resonances $f_{n,i}$ by its first component $f_{n,1}$ (fundamental resonance), following a common practice in vibration analysis.

The drivetrain is composed of two inertial elements γ_J (rotor and generator) and three gear stages (γ_{m_n}, γ_b) connected by four shafts (γ_D, γ_L), leading to 16 parameters to be scaled. The scaling factors are obtained via numerical optimization, with two objective functions shown in Eqs. (3) and (4), representing differences between reference and scaled systems. One objective function considers the safety factors for the gears, and the other one considers the normalized natural frequencies.

$$g = \left\| \boldsymbol{S}_{H,i}^{(\text{ref.})} - \boldsymbol{S}_{H,i}^{(\text{sca.})}(\gamma_{m_n}, \gamma_b) \right\|^2, \quad \boldsymbol{S}_{H,i}^{(\text{sca.})}(\gamma_{m_n}, \gamma_b) \geq S_H^{(\text{min.})} \tag{3}$$

$$h = \left(\sum_{i=1}^{N} \left| 1 - \frac{\bar{f}_{n,i}^{(\text{sca.})}(\gamma_L, \gamma_J)}{\bar{f}_{n,i}^{(\text{ref.})}} \right| \right)^2, \tag{4}$$

where $\boldsymbol{S}_H$ is a vector whose elements are the pitting safety factors for the gear-pairs on the i-th stage and $\bar{f}_{n,i}$ is the i-th normalized resonance of the system with N DOFs. The constraint in Eq. (3) means that the safety factor should be higher than a minimum $S_H^{(\text{min.})}$ and acts as a lower limit for the error in g. One could use the absolute difference between the normalized resonances instead of Eq. (4), but their relative difference led to smaller residua, and it was chosen as the objective function. One could try to combine Eqs. (3) and (4) in a single optimization problem, but the optimization algorithm (`fmincon()` by MATLAB) was not able to converge. To overcome this challenge, the full parameter set is divided into subsets, according to different aspects, e.g. per gear stage. The scaling procedure is outlined below:

(i) Scaling by stage: a single scaling factor is assigned to the normal module and face width of each gear-stage, $(\gamma_{m_n} = \gamma_b)$. The scaling factor is chosen from the optimization of Eq. (3). To preserve the tooth contact characteristic at each stage, the center distance was made proportional to the normal module.

(ii) Gear scaling (fine-tuning): at each stage, the normal module and face width have separate scaling factors, which are also chosen from the optimization of Eq. (3). One can skip the previous step and start directly with this one or use it to fine-tune the results from the first step. However, simulations shows that using both steps leads to closer agreement in terms of pitting safety factor.

(iii) Dynamic scaling: this step deals with the system's dynamic behavior by choosing scaling factors for: (1) the mass moment of inertia of rotor and generator and (2) the length of the shafts, where a single scaling factor is used for each parameter, similar to step (i). The scaling factors are chosen via optimization of Eq. (4).

(iv) Dynamic scaling (fine-tuning): separate scaling factors are assigned for each mass moment of inertia parameter and the length of each shaft, being chosen through optimization of Eq. (4). The number of scaling factors in this step (6 for the NREL 5 MW WTG) can lead to

unfeasible solutions with shaft factors with different orders of magnitude. This can be avoided by dividing the shafts into subsets with the same scaling factor. Like in step (ii), one can skip the previous step and start directly with this step or use it to fine-tune the results from step (iii). Again, the use of both steps leads to smaller residua than if only the current step is used.

The two first steps deal with the system's structural integrity and the two last ones deal with its dynamic characteristics. Steps (i) and (iii) are necessary to produce a basic scaling in terms of structural integrity and resonance distribution, with reasonable residua. The fine-tuning steps are not mandatory and can produce not feasible solutions, or increase the optimization residua from their priors. The problem's complexity is decreased by having the same scaling factor for more than one parameter. That leads to a simple procedure with an increasing level of detail, according to user needs.

Application of overall scaling factors in steps (i) and (iii) produces scaled prototypes which share geometric similarity with their reference counterpart. The other steps can produce closer agreement between the properties of interest of scaled and reference systems at the cost of distorted geometric similarity.

3. Results

The results from the application of step (i) can be seen in Fig. 2, showing that the stage scaling factor γ_S in Fig. 2(a) is proportional to the cubic root of the power scaling factor γ_P, with the third stage presenting the highest deviation from this trend. The relative difference between the pitting safety factors S_H of the scaled and reference gear stages shown in Fig. 2(b-d) has an oscillating pattern between $-15\,\%$ to $5\,\%$, with the higher absolute difference occurring in stage 1, Fig. 2(b). The figures in this section were obtained via a sweep of the power scaling factor γ_P, from 1 (5000 kW) to 0.02 (1 kW).

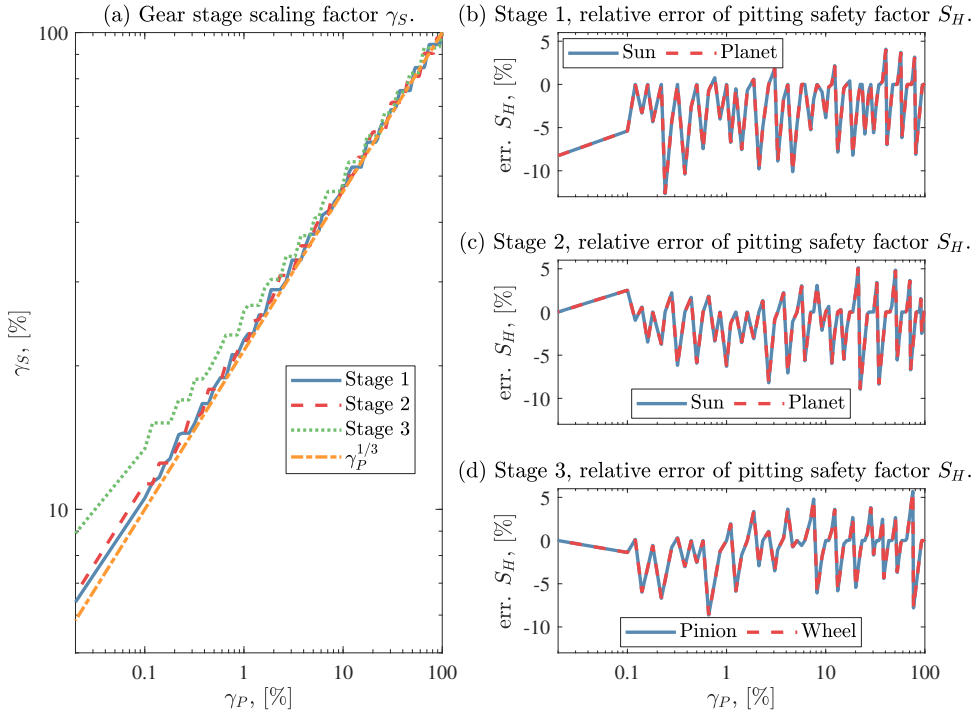

Figure 2: Outputs from step (i) according to the power scaling factor γ_P.

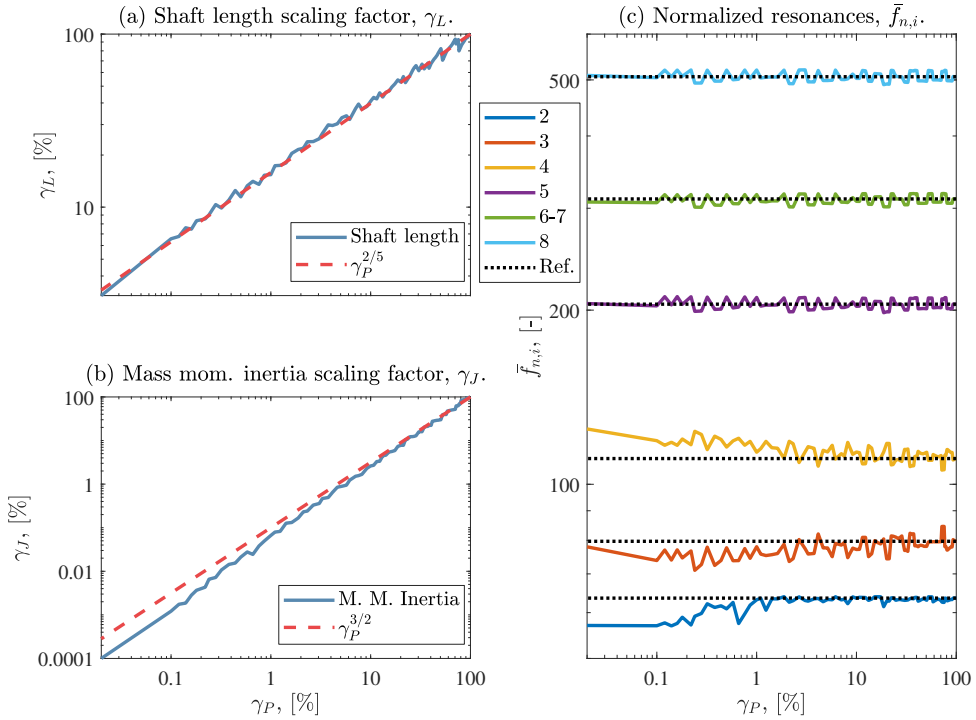

Figure 3: Outputs of steps (i) and (iii) according to the power scaling factor γ_P.

The application of steps (i) and (iii) leads to the results shown in Fig. 3, where the shaft length scaling factor γ_L is proportional to $\gamma_P^{2/5}$, while the mass moment of inertia scaling factor is proportional to the square root of γ_P^3, see Fig. 3(a-b). The normalized resonances $\bar{f}_n$ tend to oscillate around their respective reference values, represented by dotted lines in Fig. 3(c), within 12.5 % of relative difference for the three first resonances (2-4) and 3.3 % for the others.

As mentioned in Section 2, one can resume the scaling procedure after performing steps (i) and (iii), but it is also possible to improve the results obtained by those steps by assigning independent scaling factors for each parameter.

The application of steps (ii), using the scaling factors from step (i) as starting point, leads to smaller relative differences in S_H and fewer oscillations, especially for γ_P below 10 %, as shown in Fig. 4(c-e). The scaling factors for the normal module and face width for each gear stage shown in Fig. 4(a,b) also follow the same cubic root trend presented in step (i), see Fig. 2(a).

On the step (iv), to decrease the problem's complexity and avoid unfeasible solutions, the shaft length parameters are grouped into pairs with the same scaling factor and the rotor and generator have the same scaling factor for their mass moment of inertia. Different shaft combinations are possible and can produce a similar cubic root trend for the shaft's scaling factors. However it is also possible to have combinations that produce unfeasible results. On the extreme cases were each parameter has its own scaling factor, one cannot observe any form of trend between the parameters scaling factors and the power scaling factor γ_P. That suggests that when taken independently, the scaling factors are more sensitive to γ_P than when they are bound to vary in groups as in steps (i) and (iii).

The results from the down-scaling procedure using steps (i) to (iv) are shown in Fig. 5. The low-speed (LSS) and high-speed (HSS) shafts have the same scaling factor, while the intermediate speed (ISS) and the high-speed intermediate shaft (HSIS) have the same scaling factor. Comparing with the results from steps (i) and (iii) in Fig. 3, one can see that the resonances are closer to their reference values (black dotted lines), presenting 6 % of relative

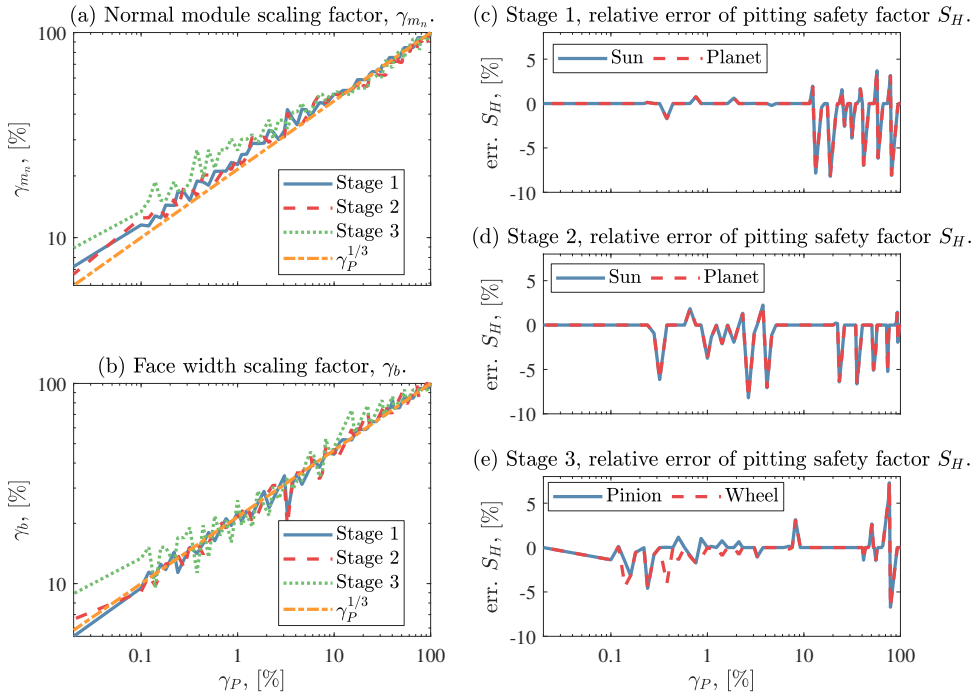

Figure 4: Outputs of steps (i) to (iii) according to the power scaling factor γ_P.

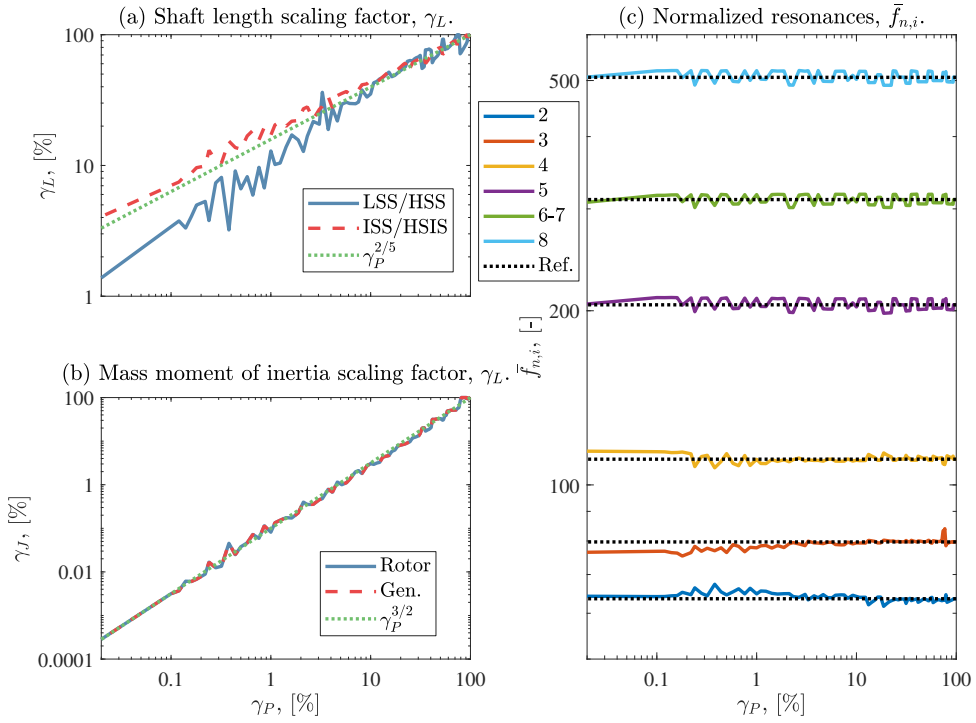

Figure 5: Outputs from steps (i) to (iv) according to the power scaling factor γ_P.

variation.

4. Quantitative cross-scale comparison

Results from down-scaling the NREL 5 MW WTG to 500 kW (10 %), 50 kW (1 %), 5 kW (0.1 %), and 0.5 kW (0.01 %) are shown in Table 1. The procedure described in Section 2 using steps (i) to (iv) led to down-scaled WTGs with similar characteristics as their full-scale reference, with relative deviations for the pitting safety factors and normalized resonances being restricted to 3.7 %. The highlighted values (inside boxes) in Table 1 are those with a higher deviation from the reference WTG. Only the 5 kW WTG was not able to match all of the pitting safety factors of its 5000 kW reference. For the normalized resonances, the higher deviations occurred for its second and third values.

Table 1: Safety factors and normalized resonances for the NREL WTGB at different power scales. The terms inside boxes present higher deviation from the reference.

Rated power, (kW)	Pitting safety factors						Normalized resonances, $\bar{f}_{n,i}$					
	Stage 1		Stage 2		Stage 3		2	3	4	5	6-7	8
5000	1.34	1.32	1.65	1.80	1.83	1.88	63.57	79.70	110.78	204.78	311.31	506.35
500	1.34	1.32	1.65	1.80	1.83	1.88	64.16	79.38	110.33	203.04	308.34	502.22
50	1.34	1.32	1.65	1.80	1.83	1.88	65.32	77.87	109.76	209.94	317.83	519.08
5	1.34	1.32	1.65	1.80	1.86	1.90	64.11	76.77	114.13	210.76	316.61	519.74
0.5	1.34	1.32	1.65	1.80	1.83	1.88	65.02	77.12	114.10	211.34	316.23	519.11
	Relative deviation, (%)											
500	0.00	0.00	0.00	0.00	0.00	0.00	-0.93	0.39	0.40	0.85	0.96	0.82
50	0.00	0.00	0.00	0.00	0.00	0.00	-2.76	2.29	0.92	-2.52	-2.09	-2.51
5	0.00	0.00	0.00	0.00	-1.38	-1.38	-0.86	3.67	-3.02	-2.92	-1.70	-2.64
0.5	0.00	0.00	0.00	0.00	0.00	0.00	-2.29	3.23	-3.00	-3.20	-1.58	-2.52

Comparing the relative deviations for the safety factors and normalized resonances, the closer agreement obtained by the safety factors can be explained by its dependence on only two parameters for each stage and being optimized before the normalized resonances.

5. Conclusions

This work presents a straightforward procedure to down-scale multi-stage drivetrains that can be used as the first step when designing a lab-scaled version of an industrial-scale system. The NREL 5 MW drivetrain [13] is down-scaled to different fractions (e.g. 10 %, 0.1 % and 0.01 %) of its rated power while minimizing variations of its structural safety and resonance distribution. The complexity and computational cost of the scaling problem is decreased by subdividing the parameters to be scaled according to their influence on the system's properties of interest. The system's integrity level and resonance distribution are preserved via the execution of specific steps, providing an initial overall scaling of the drivetrain. This first scaling can be used as an starting point to further steps developed to obtain closer agreement between the properties of full-scale and small-scale equipment.

The limited relative deviations presented in Table 1 (all below 4 %) indicate the viability of the proposed methodology for down-scaling complex machines. Scaling relations between the WTG rated power and the gear's normal module, face width and the shaft's length were fitted from simulated data and can serve as the initial step to design down-scaled WTG testing facilities.

This work can be expanded in several ways. One can analyze the influence of varying the rotor speed together with the rated power; include other failure modes, such as tooth root bending, on the down-scaling analysis; or choose another system property (e.g. vulnerability map) to be preserved. These would benefit from the use of multi body systems models, taking the system's radial dynamics into account. Those developments can improve our understanding of how complex machines behave and fail, leading to more efficient design, testing, and monitoring practices.

Appendix – Drivetrain and its Mathematical model

The NREL 5 MW reference WT was presented by [17] and its reference gearbox was proposed by [13], consisting of three stages (2 planetary and 1 parallel), as shown in Fig. 1. Some of its parameters are shown in Table 2. The other parameters do not suffer any change and their values can be found on [13]. The dimensions of the shafts at each stage can be seen in Table 3.

Table 2: Dynamic properties of the NREL 5 MW drivetrain. Taken from [13].

Parameter	To scale?	Stage 1	Stage 2	Stage 3	Unit
Type	—	Planetary	Planetary	Parallel	—
Number of planets	No	3	3	—	—
Normal module	Yes	45	21	14	mm
Face width	Yes	491	550	360	mm
Center distance	Indirect	863	584	861	mm
Mass mom. inertia* (sun/pinion)	Yes	225.47	8.84	3.72	kgm^2
Mass mom. inertia* (planet/wheel)	Yes	156.92	139.94	942.89	kgm^2
Mass mom. inertia* (ring gear)	Yes	14.9×10^3	6.6×10^3	—	kgm^2
Mass mom. inertia* (carrier)	Yes	10.5×10^3	2.47×10^3	—	kgm^2

* estimated

Table 3: Shaft dimensions of the NREL 5 MW drivetrain.

Parameter	To scale?	*LSS*	*ISS*	*HSIS*	*HSS*	Unit
Diameter	Yes	700	533	333	333	mm
Length	Yes	2000	500	666	1000	mm

A lumped parameter model is used to represent the system's torsional dynamic behavior, see Fig. 1, ignoring its radial components. Local inertia and stiffness matrices are obtained for each stage of the gearbox and for each shaft. The internal torsional dynamics of each gear stage is modeled following [16], where each planetary stage has 5 degrees-of-freedom (DOFs) (carrier, 3 planets, and sun) and the parallel stage has two DOFs. For the i-th planetary stage:

$$\boldsymbol{\theta} = \begin{bmatrix} \theta_{c_i} & \theta_{p_{i1}} & \theta_{p_{i2}} & \theta_{p_{i3}} & \theta_{s_i} \end{bmatrix}, \quad \boldsymbol{M} = \mathrm{diag}(\begin{bmatrix} m_c a_w^2 & m_p r_p^2 & m_p r_p^2 & m_p r_p^2 & m_s r_s^2 \end{bmatrix}), \tag{5}$$

$$\boldsymbol{K} = \begin{bmatrix} 3a_w^2(k_{rp}+k_{sp}) & a_w r_p(k_{rp}-k_{sp}) & a_w r_p(k_{rp}-k_{sp}) & a_w r_p(k_{rp}-k_{sp}) & -3a_w r_s k_{sp} \\ & r_p^2(k_{rp}+k_{sp}) & 0 & 0 & r_p r_s k_{sp} \\ & & r_p^2(k_{rp}+k_{sp}) & 0 & r_p r_s k_{sp} \\ & & & r_p^2(k_{rp}+k_{sp}) & r_p r_s k_{sp} \\ \text{Symmetric} & & & & 3r_s^2 k_{sp} \end{bmatrix}, \tag{6}$$

where sun, planet, ring and carrier terms are represented by the subscripts s, p, r and c. The mass, reference radius and angular position of those elements are represented by m, r and, θ, while a_w accounts for the center distance. The meshing stiffness of ring-planet and sun-planet gear pairs are constant, being represented by k_{rp} and k_{sp}, respectively. Similarly, for the parallel stage:

$$\boldsymbol{\theta} = \begin{bmatrix} \theta_W & \theta_P \end{bmatrix}, \qquad \boldsymbol{M} = \mathrm{diag}(\begin{bmatrix} m_W r_W^2 & m_P r_P^2 \end{bmatrix}), \qquad \boldsymbol{K} = k_{PW} \begin{bmatrix} r_W^2 & r_P r_W \\ r_P r_W & r_P^2 \end{bmatrix}, \tag{7}$$

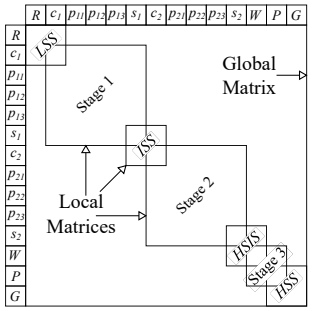

Figure 6: Illustration of assembly process of global matrices from local matrices of shaft and gear stages.

where pinion and wheel terms are represented by the subscripts P and W. The constant meshing stiffness of the pinion-wheel gear pair is represented by k_{PW}. For each shaft:

$$\boldsymbol{\theta} = \begin{bmatrix} \theta_a & \theta_b \end{bmatrix}, \qquad \boldsymbol{M} = \frac{mD^2}{48}\begin{bmatrix} 2 & 1 \\ 1 & 2 \end{bmatrix}, \qquad \boldsymbol{K} = \frac{\pi G D^4}{32L}\begin{bmatrix} 1 & -1 \\ -1 & 1 \end{bmatrix}, \tag{8}$$

where m, D, L and G represent the shaft's mass, diameter, length, and shear modulus of its material. The subscripts a and b represent the rotation at the shaft's left and right ends, e.g. on the low-speed shaft in Fig. 1 represented by k_{LSS}, one has $a = R$ and $b = c1$. The global mass and stiffness matrices are assembled according to Fig. 6, resulting in a 14 DOF model accounting for rotations of the gears as well as the rotor and generator, R and G.

References

[1] NREL 2020 Dynamometer research facilities URL https://www.nrel.gov/wind/facilities-dynamometer.html
[2] CENER 2017 Powertrain test laboratories and electrical testing URL http://www.cener.com/en/wind-turbine-test-laboratory-lea/powertrain-test-laboratories-and-electrical-testing/
[3] Clemson University SCE&G Energy Innovation Center 2020 Wind turbine test beds URL https://clemsonenergy.com/wind-turbine-test-beds/
[4] Musial W, Beiter P and Spitsen P Nunemaker J G V 2019 2018 offshore wind technologies market report Tech. rep. U.S. Department of Energy Washington, USA
[5] Casaburo A, Petrone G, Franco F and De Rosa S 2019 *Applied Mechanics Reviews* **71** 030802
[6] Viselli A M, Goupee A J and Dagher H J 2015 *Journal of Offshore Mechanics and Arctic Engineering* **137**
[7] Gasch R and Twele J 2012 Scaling wind turbines and rules of similarity *Wind Power Plants* (Berlin, Heidelberg: Springer Berlin Heidelberg) pp 257–271
[8] Esteban E, Salgado O, Iturrospe A and Isasa I 2017 *Mechatronics* **47** 14–23
[9] Varais A, Roboam X, Lacressonnière F, Turpin C, Cabello J, Bru E and Pulido J 2019 *Mathematics and Computers in Simulation* **158** 65–78
[10] Lim C W 2017 *International Journal of Precision Engineering and Manufacturing - Green Technology* **4** 409–418 ISSN 21980810
[11] Lim C W 2019 *Renewable Energy* **144** 68–76 ISSN 18790682
[12] Oh K Y, Lee J K, Bang H J, Park J Y, Lee J S and Epureanu B 2014 *Renewable Energy* **62** 379–387 ISSN 09601481
[13] Nejad A R, Guo Y, Gao Z and Moan T 2016 *Wind Energy*
[14] ISO 2019 Calculation of load capacity of spur and helical gears – part 2: Calculation of surface durability (pitting) Standard ISO 6336-2:2019 International Organization for Standardization Geneva, Switzerland URL https://www.iso.org/standard/63821.html
[15] Budynas R G and Nisbett J K 2015 *Shigley's mechanical engineering design* 10th ed (McGraw-Hill)
[16] Kahraman A 1994 *Journal of Sound and Vibration* **173** 125–130
[17] Jonkman J, Butterfield S, Musial W and Scott G 2009 Definition of a 5-MW reference wind turbine for offshore system development Tech. Rep. NREL/TP-500-38060 National Renewable Energy Laboratory